PTEP

Prog. Theor. Exp. Phys. **2019**, 083E01 (14 pages)
DOI: 10.1093/ptep/ptz074

Deformation of neutron stars due to poloidal magnetic fields

K. Yanase[1,*], N. Yoshinaga[1], E. Nakano[2], and C. Watanabe[1]

[1]*Department of Physics, Saitama University, Saitama City 338-8570, Japan*
[2]*Department of Physics, Kochi University, Kochi City 780-8520, Japan*
*E-mail: yanase@nuclei.th.phy.saitama-u.ac.jp

Received September 21, 2018; Revised June 7, 2019; Accepted June 8, 2019; Published August 11, 2019

The mass–radius (MR) relation of deformed neutron stars in the axially symmetric poloidal magnetic field is calculated. The MR relation is obtained by solving the Hartle equations, whereas the one for spherical stars is obtained by the Tolman–Oppenheimer–Volkoff equations. The anisotropic effects of the poloidal magnetic fields are found to be non-negligible for a strong magnetic field more than 3×10^{18} G at the center of a neutron star.

Subject Index E32

1. Introduction

Recent observational studies of binary systems have revealed that there are at least two pulsars with masses of around $2M_\odot$, PSR J1614−2230 [1] and PSR J0348+0432 [2], within errors of a few %. These pulsars are remarkably massive compared to typical neutron stars with masses of $1.4M_\odot$ on average. The presence of such massive neutron stars can be easily explained if the neutron star matter consists of only nucleons and some varieties of leptons. However, hyperons should appear naturally in the high-density region of the neutron star where its density is a few times higher than the nuclear saturation density. The appearance of hyperons softens the equation of states (EoS) of neutron star matter, and makes it difficult to explain the presence of massive neutron stars. This problem is referred to as the hyperon puzzle. Various kinds of EoSs have been developed in the Hartree–Fock method [3,4], relativistic mean field theories [5–9], chiral effective field theories [10–12], and quantum Monte Carlo approaches [13–15].

Other observational discoveries of soft γ-ray repeaters (SGRs) and anomalous X-ray pulsars (AXPs) have indicated that these pulsars have strong magnetic fields of around 10^{14}–10^{15} G on the surface assuming that magnetic fields are radiated in a dipole manner. Pulsars with such strong magnetic fields are called magnetars. Twenty-nine magnetars and their candidates are known so far [16]. However, massive neutron stars may not be magnetars.

These observations motivate us to theoretically study the effects of strong magnetic fields on the EoS of the neutron star matter, and eventually on the mass–radius (MR) relation of neutron stars. There are a lot of preceding works on the effects of Pauli paramagnetism and Landau diamagnetism on the EoS and the MR relations of neutron stars [17–20], quark stars [21,22], and hybrid stars [23,24] in the presence of strong magnetic fields.

© The Author(s) 2019. Published by Oxford University Press on behalf of the Physical Society of Japan.
This is an Open Access article distributed under the terms of the Creative Commons Attribution License (http://creativecommons.org/licenses/by/4.0/), which permits unrestricted reuse, distribution, and reproduction in any medium, provided the original work is properly cited.

Downloaded from https://academic.oup.com/ptep/article-abstract/2019/8/083E01/5546028 by CERN - European Organization for Nuclear Research user on 07 September 2019

In these studies they argued that the presence of strong magnetic fields makes the EoS of the neutron star matter stiffer, so that neutron stars could have larger masses compared with the mass without magnetic fields. It was shown that the mass of a neutron star can exceed $2M_\odot$ if the magnetic field strengths at the centers of the neutron stars become of the order of 10^{18} G. They adopted isotropic forms of pressure to calculate the MR relation of neutron stars using the Tolman–Oppenheimer–Volkoff (TOV) equations, which might not be valid for anisotropic magnetic fields. In fact it is unrealistic that magnetic fields generate an isotropic pressure since the energy–stress tensor components due to a magnetic field depend on the direction of the magnetic field. An anisotropic energy–stress tensor should be considered depending on realistic magnetic field configurations.

It has been shown that either toroidal or poloidal magnetic fields alone would become unstable in non-rotating stars [25,26]. Moreover, recent studies on magnetic field configurations have indicated that magnetic fields in neutron stars have both poloidal and toroidal components. The energy of the poloidal component E_p as a fraction of the total magnetic field energy E is numerically evaluated as $E_p/E \leq 0.8$ [27,28]. The anisotropic configuration of magnetic fields affects the deformations of neutron stars so that one should solve the Einstein equation in the presence of anisotropic fields. There are a few numerical works calculating the MR relations with anisotropic magnetic pressures [29,30]. For a magnetic field produced by a certain electric current distribution, they solved the Einstein equation in axially symmetric space.

In this paper we consider the deformation of neutron stars due to poloidal magnetic fields (PMFs) and calculate the MR relations of neutron stars. The anisotropic effects of the PMF on the energy–stress tensor are assumed to be small compared to the matter components. Under this assumption, a perturbative approach for the metric is adopted up to second order of the magnetic field strength. The perturbative terms of the metric provide the additional mass and the eccentricity for deformed objects. This perturbative approach was originally introduced for slowly rotating neutron stars by J. B. Hartle and others [31–34]. R. Mallick et al. applied this formulation to the calculation of the additional mass and the eccentricity of deformed neutron stars due to strong magnetic fields [35]. They used a few kinds of EoSs without considering Landau diamagnetism and anomalous magnetic moments (AMMs). We take into account the above effects, which enable us to discuss quantitatively the question of whether $2M_\odot$ is realized in the realistic EoS or not. We discuss to what extent the anisotropy and the magnetic effects on the EoS play important roles in the question of whether neutron stars can exceed $2M_\odot$.

This paper is organized as follows. In Sect. 2, the frameworks of the calculation of EoSs and the Hartle equations for a deformed metric in the presence of magnetic fields are presented. In Sect. 3, numerical results are given. In Sect. 4, some discussions related to the treatment of magnetic fields are given. Also a significant correlation between the neutron star radius and the slope of the symmetry energy is discussed. Finally the results are summarized in Sect. 5.

2. Formulations

2.1. Equation of state

In this paper the neutron star matter is assumed to be static and uniform in the high-density region, which is described in the relativistic mean field (RMF) theory based on the nonlinear Walecka model. The Lagrangian is given as [5–7,9,17,20,24,36]

$$\mathcal{L} = \sum_b \mathcal{L}_b + \mathcal{L}_m + \sum_l \mathcal{L}_l + \mathcal{L}_{\rm em}, \tag{1}$$

Downloaded from https://academic.oup.com/ptep/article-abstract/2019/8/083E01/5546028 by CERN - European Organization for Nuclear Research user on 07 September 2019

where

$$\mathcal{L}_b = \overline{\psi}_b \left(i\gamma_\mu \partial^\mu - m_b + g_{\sigma b}\sigma + g_{\sigma^* b}\sigma^* - g_{\omega b}\gamma_\mu \omega^\mu - g_{\phi b}\gamma_\mu \phi^\mu - g_{\rho b}\gamma_\mu \boldsymbol{\tau}\cdot\boldsymbol{\rho}^\mu \right.$$
$$\left. - q_b \gamma_\mu A^\mu - \kappa_b \sigma_{\mu\nu} F^{\mu\nu} \right) \psi_b, \tag{2}$$

$$\mathcal{L}_m = \frac{1}{2}\left(\partial_\mu \sigma \partial^\mu \sigma - m_\sigma^2 \sigma^2\right) + \frac{1}{2}\left(\partial_\mu \sigma^* \partial^\mu \sigma^* - m_{\sigma^*}^2 \sigma^{*2}\right)$$
$$+ \frac{1}{2} m_\omega^2 \omega_\mu \omega^\mu - \frac{1}{4}\Omega_{\mu\nu}\Omega^{\mu\nu} + \frac{1}{2} m_\phi^2 \phi_\mu \phi^\mu - \frac{1}{4}\Phi_{\mu\nu}\Phi^{\mu\nu}$$
$$+ \frac{1}{2} m_\rho^2 \boldsymbol{\rho}_\mu \cdot \boldsymbol{\rho}^\mu - \frac{1}{4}\boldsymbol{P}^{\mu\nu}\cdot\boldsymbol{P}_{\mu\nu}$$
$$- \frac{1}{3} b m_n (g_\sigma \sigma)^3 - \frac{1}{4} c (g_\sigma \sigma)^4 + \frac{1}{4!}\xi \left(g_\omega^2 \omega_\mu \omega^\mu\right)^2 + \Lambda_\omega \left(g_\omega^2 \omega_\mu \omega^\mu\right)\left(g_\rho^2 \boldsymbol{\rho}_\mu \cdot \boldsymbol{\rho}^\mu\right), \tag{3}$$

$$\mathcal{L}_l = \overline{\psi}_l \left(i\gamma_\mu \partial^\mu - q_l \gamma_\mu A^\mu - m_l \right) \psi_l, \tag{4}$$

$$\mathcal{L}_{\rm em} = -\frac{1}{4} F^{\mu\nu} F_{\mu\nu}. \tag{5}$$

Here b, m, l, and em indicate baryons, mesons, leptons, and photons, respectively. The field strengths are explicitly given as

$$F_{\mu\nu} = \partial_\mu A_\nu - \partial_\nu A_\mu, \tag{6}$$

$$\Omega_{\mu\nu} = \partial_\mu \omega_\nu - \partial_\nu \omega_\mu, \tag{7}$$

$$\Phi_{\mu\nu} = \partial_\mu \phi_\nu - \partial_\nu \phi_\mu, \tag{8}$$

$$\boldsymbol{P}_{\mu\nu} = \partial_\mu \boldsymbol{\rho}_\nu - \partial_\nu \boldsymbol{\rho}_\mu - g_\rho \boldsymbol{\rho}_\mu \times \boldsymbol{\rho}_\nu. \tag{9}$$

Here, $\boldsymbol{\tau}/2$ represents the isospin operator and $\sigma_{\mu\nu} = \frac{i}{2}\left[\gamma_\mu, \gamma_\nu\right]$. The baryon octet $\{p, n, \Lambda, \Sigma^0, \Sigma^\pm, \Xi^0, \Xi^-\}$, the electron, and the muon are taken into account for fermions.

In this model, the scalar meson σ, the vector meson ω, and the vector–isovector meson ρ with masses of $m_\sigma = 511.198$ MeV, $m_\omega = 783.0$ MeV, and $m_\rho = 770.0$ MeV are introduced. The coupling constants of nucleons with these mesons, $g_{\sigma N}$, $g_{\omega N}$, and $g_{\rho N}$, and some self-interactions among mesons are determined by fitting the physical quantities at the saturation density [5,6,36]. The obtained coupling constants are listed in Table 1. The coupling constants of hyperons with these mesons and hidden-strangeness mesons, σ^* and ϕ^μ, are determined by fitting the properties of hypernuclei in the quark model [9]. In the GM1 parameter set $R_{\sigma h} = g_{\sigma h}/g_{\sigma N} = 0.6$, $R_{\omega h} = g_{\omega h}/g_{\omega N} = 0.653$, and $R_{\rho h} = g_{\rho h}/g_{\rho N} = 0.6$ are adopted. As for other couplings of hyperons with the vector and vector–isovector mesons, the SU(6) values are adopted in the TM1-a and TM2$\omega\rho$-a parameter sets:

$$R_{\omega\Lambda} = \frac{2}{3}, \quad R_{\omega\Sigma} = \frac{2}{3}, \quad R_{\omega\Xi} = \frac{1}{3}, \tag{10}$$

$$R_{\rho\Sigma} = 2, \quad R_{\rho\Xi} = 1, \tag{11}$$

$$R_{\phi\Lambda} = -\frac{\sqrt{2}}{3}, \quad R_{\phi\Sigma} = -\frac{\sqrt{2}}{3}, \quad R_{\phi\Xi} = -\frac{2\sqrt{2}}{3}. \tag{12}$$

In the TM1-b and TM2$\omega\rho$-b parameter sets, $R_{\omega\Lambda} = 1$ is adopted, which corresponds to the symmetry breaking of SU(6). Recent studies on hypernuclei provide the single-particle potentials of hyperons

Downloaded from https://academic.oup.com/ptep/article-abstract/2019/8/083E01/5546028 by CERN - European Organization for Nuclear Research user on 07 September 2019

Table 1. Coupling constants of nucleon–meson interactions.

	GM1	TM1	TM2$\omega\rho$
g_σ	8.895	10.03	9.998
g_ω	10.61	12.61	12.50
g_ρ	8.195	9.264	11.30
$b \times 10^3$	2.947	−1.508	−1.763
$c \times 10^3$	−1.070	0.061	−0.790
ξ	0	0.0169	0.0113
Λ_ω	0	0	0.03

Table 2. Baryon masses (m_b) in units of MeV, anomalous magnetic moments (κ_b), and electric charges (q_b) for the baryon octet. κ_b is defined as $\kappa_b = \mu_b/\mu_N - \mathrm{sgn}(q_b)\, m_p/m_b$ where μ_N is the nuclear magneton [43].

	p	n	Λ	Σ^+	Σ^0	Σ^-	Ξ^0	Ξ^-
m_b	938.3	939.6	1116	1189	1193	1197	1314	1321
κ_b	1.79	−1.91	−0.61	1.67	1.61	−0.38	−1.25	0.06
q_b	+1	0	0	+1	0	−1	0	−1

in the symmetric nuclear matter. The values of $U_\Lambda^N = -30$ MeV, $U_\Sigma^N = 0$ MeV, and $U_\Xi^N = -14$ MeV are adopted to determine the value of $R_{\sigma h}$. An empirical value of the binding energy in double-Λ hypernuclei $\Delta B = 0.50$ MeV is employed for adjusting the coupling of the Λ hyperon with the σ^* meson [9]. Due to the absence of information on the double-Σ and double-Ξ hypernuclei, the coupling of the Σ and Ξ hyperons with the σ^* meson is fixed to zero: $R_{\sigma^*\Sigma} = R_{\sigma^*\Xi} = 0$. Masses and charges of the baryon octet are given in Table 2. The experimental values of the anomalous magnetic moments (AMMs) defined by $\kappa_b = \mu_b/\mu_N - \mathrm{sgn}(q_b)\, m_p/m_b$ for baryons are also given.

The RMF EoS is used to describe the denser region, where its density is over the neutron drip density $\rho_{\mathrm{ND}} = 2.51 \times 10^{-4}$ fm^{-3}. The neutron drip density is predicted by the HFB-25 Brussels–Montreal nuclear mass model [37]. The neutron drip density might be changed in the presence of a strong magnetic field, but the MR relations of neutron stars are not so sensitive to the neutron drip density. In order to describe the lower-density region, the Baym–Pethick–Sutherland (BPS) EoS is used [38] with the atomic masses given in AME2012 [39,40] and HFB-24 [41].

In this paper we adopt a density-dependent magnetic field strength given by [24,42]

$$B(\rho) = B_s + B_0 \left[1 - \exp\left\{ -\alpha \left(\frac{\rho}{\rho_0} \right)^\gamma \right\} \right], \tag{13}$$

where B_s indicates the strength on the surface and and B_0 indicates that in a much denser region than that of the saturation number density ρ_0 (0.153 fm^{-3}). Here the parameters $\alpha = 0.05$ and $\gamma = 2$ are adopted [24]. In the following the value of B_s is fixed constant at 10^{15} G. Details of how to obtain the EoS in the presence of strong magnetic fields are given in Appendix A.

2.2. *Hartle equations for deformed metrics due to magnetic fields*

A theoretical method to calculate masses and eccentricities of axially deformed objects due to slow rotations was first introduced by J. B. Hartle and others in Refs. [31–34] in the framework of general relativity. The metric for such an object can be written as

Downloaded from https://academic.oup.com/ptep/article-abstract/2019/8/083E01/5546028 by CERN - European Organization for Nuclear Research user on 07 September 2019

$$ds^2 = -e^{\nu}\left[1 + 2\left\{h_0 + h_2 P_2(\cos\theta)\right\}\right]dt^2 + e^{\lambda}\left[1 + \frac{2e^{\lambda}}{r}\left\{m_0 + m_2 P_2(\cos\theta)\right\}\right]dr^2$$
$$+ r^2\left[1 + 2k_2 P_2(\cos\theta)\right]\left[d\theta^2 + \sin^2\theta\,(d\phi - \omega dt)^2\right], \tag{14}$$

where $\omega(r,\theta)$ represents the local angular velocity of a rotating star, and $h_0(r)$, $h_2(r)$, $m_0(r)$, $m_2(r)$, and $k_2(r)$ are the second-order perturbative terms with respect to the angular velocity Ω. The second-order Legendre polynomial is given as $P_2(\cos\theta) = \frac{1}{2}(3\cos^2\theta - 1)$.

In this paper, non-rotating stars are treated so that only deformations are taken into account due to the poloidal magnetic fields $\boldsymbol{B} = B\boldsymbol{e}_z$, where the strength B is given by Eq. (13). This indicates that $\omega(r,\theta) = 0$ and now the perturbative expansion parameter is the magnetic field strength B rather than Ω. In the following all the physical quantities are treated up to the second order of the strength B.

The total pressure is given by

$$p = p_0 + \delta p, \tag{15}$$

where p_0 is the matter contribution, and the angular dependence of the perturbative magnetic pressure δp is given by

$$\delta p = \delta p_0 + \delta p_2 P_2(\cos\theta), \tag{16}$$

$$\delta p_0 = \frac{1}{3}\frac{B^2}{2}, \quad \delta p_2 = -\frac{4}{3}\frac{B^2}{2}. \tag{17}$$

If the magnetic pressure δp is much smaller than the matter contribution p_0, the total energy density $\varepsilon(p)$ can be expanded as

$$\varepsilon(p_0 + \delta p) = \varepsilon(p_0) + \left.\frac{d\varepsilon}{dp}\right|_{p=p_0}\delta p. \tag{18}$$

It was shown that the magnetization of protons and neutrons for the neutron star matter is at most two orders of magnitude smaller than the magnetic field strength in the strong magnetic fields of 10^{15-18} G [19,20]. Thus the contribution of the magnetization to the magnetic pressure can be neglected.

The unperturbed part of the Einstein equation

$$G^{\mu\nu} \equiv R^{\mu\nu} - \frac{1}{2}g^{\mu\nu}R = 8\pi T^{\mu\nu} \tag{19}$$

becomes the TOV equations

$$\frac{dM_0}{dr} = 4\pi r^2 \varepsilon(p_0), \tag{20}$$

$$\frac{dp_0}{dr} = -\frac{(\varepsilon(p_0) + p_0)\left(M_0 + 4\pi r^3 p_0\right)}{r\,(r - 2M_0)}, \tag{21}$$

where the zeroth-order parts of the metric are given by

$$\frac{d\nu}{dr} = -\frac{2}{\varepsilon(p_0) + p_0}\frac{dp_0}{dr}, \tag{22}$$

$$e^{-\lambda} = 1 - \frac{2M_0}{r}. \tag{23}$$

Downloaded from https://academic.oup.com/ptep/article-abstract/2019/8/083E01/5546028 by CERN - European Organization for Nuclear Research user on 07 September 2019

The Hartle equations [31,33,34] consisting of the second-order terms of the Einstein equation are given by

$$\frac{dm_0}{dr} = 4\pi r^2(\varepsilon(p_0)+p_0)\left.\frac{d\varepsilon}{dp}\right|_{p=p_0}\delta F_0, \tag{24}$$

$$\frac{d}{dr}\delta F_0 = -m_0 e^{2\lambda}\left(8\pi p_0 + \frac{1}{r^2}\right) - 4\pi r e^{\lambda}(\varepsilon(p_0)+p_0)\delta F_0, \tag{25}$$

$$\frac{dk_2}{dr} = \frac{4}{r(r-2M_0)\nu'}k_2 + \frac{4r}{(r-2M_0)\nu'}\left\{\frac{4}{r^2}+\frac{4M_0}{r^3}-8\pi(\varepsilon(p_0)+p_0)\right\}\delta F_0, \tag{26}$$

where $\nu' = d\nu/dr$. Here δF_0 is defined indirectly through

$$\begin{aligned} F(p) &\equiv \log(\varepsilon(p)+p) - \int_{\varepsilon_c}^{\varepsilon(p)}\frac{1}{\varepsilon+p}d\varepsilon \\ &= F_0 + \delta F_0 + \delta F_2 P_2(\cos\theta), \end{aligned} \tag{27}$$

where δF_0 and δF_2 are second-order terms in B, and F_0 is the zeroth-order term, independent of B. The symbols F, F_0, δF_0, δF_2 were originally denoted as P, P_0, δP_0, δP_2 in Ref. [34], but to avoid descriptive confusions, different notations are adopted here. This definition of $F(p)$ is equivalent to

$$dF = \frac{1}{\varepsilon(p)+p}dp, \tag{28}$$

implying that δF_0 and δF_2 are given through δp_0 and δp_2 in Eq. (17) as

$$\delta F_0 = \frac{1}{\varepsilon(p)+p}\delta p_0, \quad \delta F_2 = \frac{1}{\varepsilon(p)+p}\delta p_2. \tag{29}$$

The Hartle equations and the EoS for the neutron star matter should be solved simultaneously, but the strength of B can depend on the number density ρ in the EoS whereas dependence on r is required in the Hartle equations. In this paper, a density-dependent form of the magnetic field (Eq. (13)) is adopted instead of solving Eq. (25), so that Eqs. (24) and (26) are solved simultaneously.

The total mass of a neutron star up to the second order of B is the sum of the unperturbed mass M_0 and the additional mass m_0, which are calculated by the TOV equations and the Hartle equations, respectively. The eccentricity is defined by [33,34]

$$e = \sqrt{\left(\frac{R_{\rm e}}{R_{\rm p}}\right)^2 - 1}, \tag{30}$$

where $R_{\rm e}$ and $R_{\rm p}$ represent the equatorial radius and the polar radius, respectively. The coordinate transformation $r^2 \to r^2\left[1+k_2(r)P_2(\cos\theta)\right]$ leads to an expression of eccentricity

$$e = \sqrt{-3\left(\frac{\xi_2(R)}{R}+k_2(R)\right)}, \tag{31}$$

where the isotropic radius R is defined through $p_0(R)=0$, and $\xi_2(R)$ is given by

$$\xi_2(r) = -\delta p_2(r)/\frac{dp_0}{dr}. \tag{32}$$

Downloaded from https://academic.oup.com/ptep/article-abstract/2019/8/083E01/5546028 by CERN - European Organization for Nuclear Research user on 07 September 2019

3. Numerical results

Figure 1 shows calculated mass–radius (MR) relations in the poloidal magnetic field (PMF) with a large central magnitude of $B_0 = 3 \times 10^{18}$ G for various EoSs. Here the radius indicates the equatorial radius R_e in the PMF case whereas the radius means the isotropic one R in other cases. Using the TM2$\omega\rho$-b parametrization, which provides the stiffest EoS among all the EoSs in this paper, the largest masses of observed neutron stars can be explained. For other EoSs, the mass hardly surpasses twice the solar mass.

In Fig. 2 various results are given in the two cases of spherically symmetric magnetic pressure (SSMP) and the poloidal magnetic field (PMF). MR relations without hyperons are also plotted in green. It is seen that maximum masses without hyperons surpass $2.23\mathrm{M}_\odot$. The cases without any magnetic fields are also shown for comparison. Here in the SSMP treatment, TOV equations are solved without considering the deformation, whereas in the PMF treatment the Hartle equations are solved by considering the axial deformation. As for the SSMP, the perpendicular component of the magnetic energy–stress tensor, $p_{B,\perp} = B^2/2$, is employed. The maximum masses for all the cases considered are listed in Table 3. It is apparent from Fig. 2 and Table 3 that the magnetic pressure hardly contributes to the MR relations up to $B_0 = 10^{18}$ G. In the SSMP cases, neutron stars are enlarged due to the overestimated magnetic pressure, and masses for all the EoSs exceed twice the solar mass with $B_0 = 3 \times 10^{18}$ G. However, in the PMF case, the contribution to the maximum mass from the poloidal magnetic field is suppressed in comparison with the SSMP case. In fact the mean value of the magnetic pressure arising from the PMF case is smaller by a factor of three than that obtained in the SSMP case [44,45]. In the SSMP case, the radius of a neutron star with a typical mass of $1.4\mathrm{M}_\odot$ is 13.3 km in the case of $B_0 = 10^{18}$ G, and 13.7 km for $B_0 = 3 \times 10^{18}$ G, respectively. In contrast the equatorial radius in the PMF case hardly depends on the magnitude of magnetic fields.

Figure 3 shows the eccentricity defined in Eq. (31), which represents the degree of deformation of a neutron star. For a deformed object with $e = 0.6$ (almost the largest value in our calculation), $R_p/R_e = 0.86$.

Finally, we conclude this section by discussing the validity of the perturbative approach in the PMF case. Figure 4 shows the ratio of the perturbative mass m_0 to the unperturbed mass M_0 in the radial part of the metric. The central baryon number density is $\rho = 1.0\,\mathrm{fm}^{-3}$, which gives almost the maximum mass in each case. Figure 5 shows another perturbative term $-k_2$ in the angular part of the metric. These figures imply that the perturbative prescription is well applicable at least for $B_0 = 3 \times 10^{18}$ G. As seen from Figs. 4 and 5, we obtain the small perturbative terms as $m_0(R)/M_0(R) \sim 0.1$ and $|-k_2| \sim 0.15$, so this perturbative treatment is justified.

4. Discussions

As described in the previous section, a density-dependent form of magnetic fields (Eq. (13)) was adopted instead of solving Eq. (25). We avoided solving Eq. (25) simply because in that case we should solve the EoS as a function of both baryon number density ρ and the magnetic field strength B. Numerically this is extremely difficult to carry out.

Here we adopt an eclectic method where the EoS is given in terms of the magnetic field in Eq. (13), but nevertheless the Hartle equations are solved without assuming Eq. (13). After solving the Hartle equations, we obtain the magnetic field strengths as a function of radius through Eqs. (17) and (29). In the following the magnetic field thus obtained is called the PMF-δF_0 field, while the field in Eq. (13) is called the PMF-$B(\rho)$ field. For the EoS, we have used TM2$\omega\rho$-b parametrization.

Downloaded from https://academic.oup.com/ptep/article-abstract/2019/8/083E01/5546028 by CERN - European Organization for Nuclear Research user on 07 September 2019

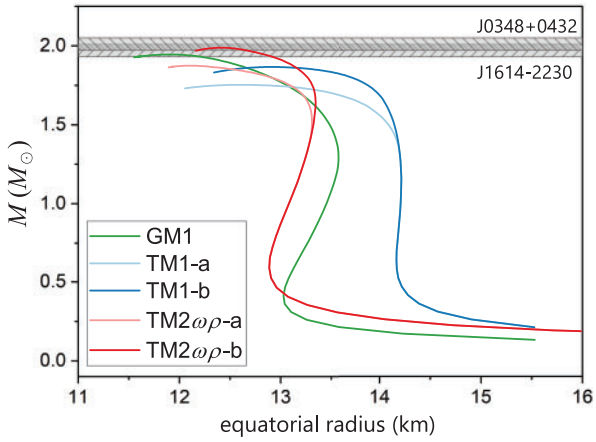

Fig. 1. MR relations for deformed neutron stars in the poloidal magnetic field (PMF) with $B_0 = 3 \times 10^{18}$ G for various EoSs. The masses of two observed massive neutron stars are illustrated by the shaded area.

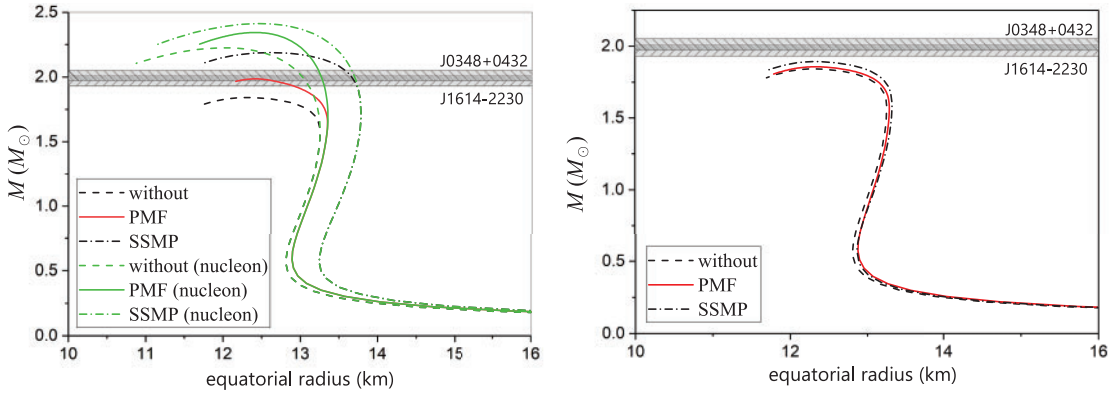

Fig. 2. MR relations with the TM2$\omega\rho$-b parametrization in the poloidal magnetic field (PMF) case, and in the spherically symmetric magnetic pressure (SSMP) case. MR relations without hyperons are plotted in green (nucleon). The central magnitudes of the magnetic fields are $B_0 = 3 \times 10^{18}$ G (left panel) and $B_0 = 10^{18}$ G (right panel), respectively. MR relations without any magnetic fields (without) are shown for comparison.

Table 3. Maximum masses in the PMF and the SSMP are listed in units of $M_\odot$. Applied magnetic field strengths are shown in the first row.

	$B_0 = 0$ G	$B_0 = 10^{18}$ G		$B_0 = 3 \times 10^{18}$ G	
		PMF	SSMP	PMF	SSMP
GM1	1.784	1.802	1.836	1.945	2.135
TM1-a	1.614	1.627	1.672	1.753	2.038
TM1-b	1.738	1.750	1.791	1.866	2.119
TM2$\omega\rho$-a	1.715	1.731	1.773	1.874	2.111
TM2$\omega\rho$-b	1.888	1.902	1.895	1.988	2.192

In Fig. 6, the PMF-δF_0 field is shown by a red line, and PMF-$B(\rho)$ ($B_0 = 3 \times 10^{18}$ G, $B_s = 10^{15}$ G, $\alpha = 0.05$, and $\gamma = 2$) is also shown as a reference by a black line. We have chosen the central baryon number density as $\rho = 1.0$ fm^{-3}. From this figure, it is seen that there is little difference between the two cases shown in PMF-δF_0 and PMF-$B(\rho)$ from the center to 5 km, but a substantial difference is seen from 5 km to 12 km, where the PMF-δF_0 field is stronger than the PMF-B(ρ) field. This figure

Downloaded from https://academic.oup.com/ptep/article-abstract/2019/8/083E01/5546028 by CERN - European Organization for Nuclear Research user on 07 September 2019

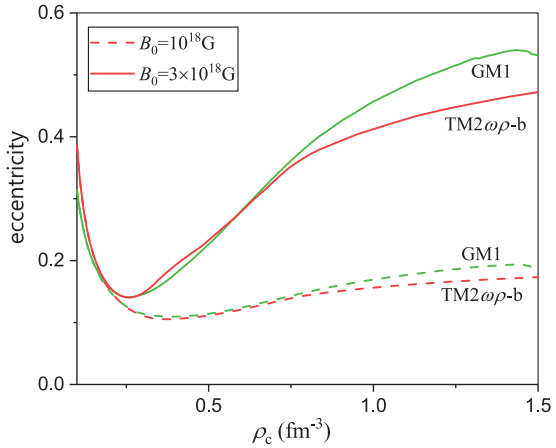

Fig. 3. Eccentricities e in Eq. (31) as functions of the central baryon number density ρ_c for GM1 and TM2$\omega\rho$-b EoSs with two kinds of magnetic field strengths ($B_0 = 3 \times 10^{18}$ G and $B_0 = 10^{18}$ G).

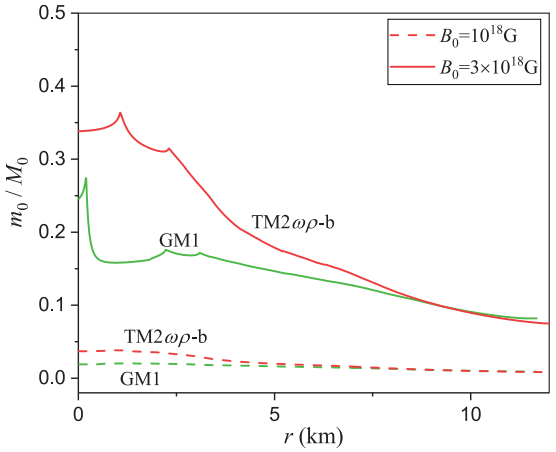

Fig. 4. Ratios of the perturbative mass term $m_0(r)$ to the unperturbed mass term $M_0(r)$ as a function of the distance from the center r for GM1 and TM2$\omega\rho$-b EoSs with two kinds of magnetic field strengths.

shows that magnetic fields obtained by solving Eq. (25) sustain strong magnetic fields continuously from the center to the surface, but they drop down suddenly only near the surface.

Figure 7 shows the MR relations with and without magnetic fields. In the presence of the magnetic fields, the mass given by the PMF-δF_0 field is shown by a red dot-dashed line and the mass obtained by PMF-$B(\rho)$ is shown by a red solid line. The dashed line indicates that without magnetic fields. The maximum mass given by PMF-δF_0 is 2.15M$_\odot$, while that by PMF-$B(\rho)$ is 1.99M$_\odot$. Due to the strong magnetic fields continuing to the surface in the PMF-δF_0 field, the perturbative term m_0 gets larger. As a result, the total mass $M = M_0(R) + m_0(R)$ in the PMF-δF_0 field becomes bigger than that by the PMF-$B(\rho)$ field.

It is interesting to investigate what properties of EoSs actually decide the radii of neutron stars. The basic nuclear properties at saturation reproduced by five EoSs are given in Table 4. These parameters refer to the binding energy B/A, the nuclear normal density ρ_0, the incompressibility K, the incompressibility of symmetry energy $K_{\rm sym}$, the symmetry energy at saturation J, and the symmetry-energy slope parameter L, respectively. It is seen in Fig. 1 and Table 4 that the slope of the

Downloaded from https://academic.oup.com/ptep/article-abstract/2019/8/083E01/5546028 by CERN - European Organization for Nuclear Research user on 07 September 2019

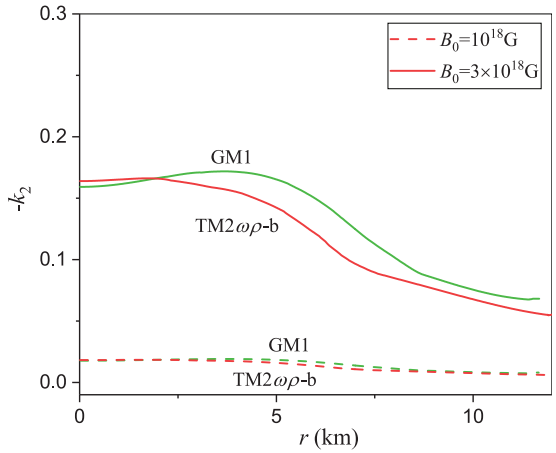

Fig. 5. The perturbative term $-k_2$ in the angular part of the metric as a function of the distance from the center r for GM1 and TM2$\omega\rho$-b EoSs with two kinds of magnetic field strengths.

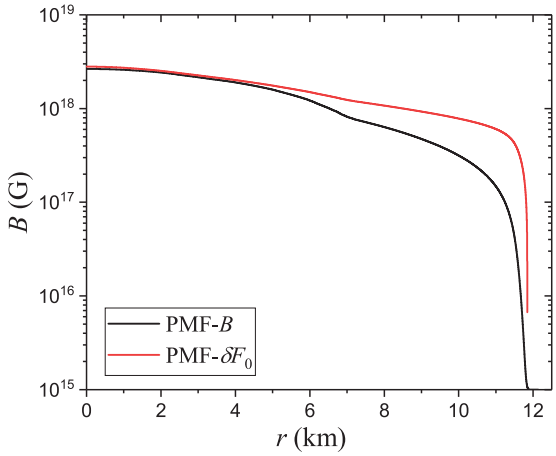

Fig. 6. The red line indicates the PMF-δF_0 field, and the black line indicates the PMF-$B(\rho)$ field ($B_0 = 3 \times 10^{18}$ G, $B_s = 10^{15}$ G, $\alpha = 0.05$, and $\gamma = 2$). The TM2$\omega\rho$-b EoS is adopted.

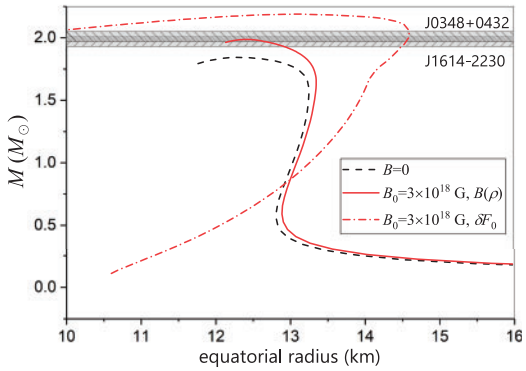

Fig. 7. MR relations using magnetic fields solving Eq. (25) (red dot-dashed line, PMF-δF_0) and the magnetic field in Eq. (13) (red solid line, PMF-B(ρ)). The TM2$\omega\rho$-b EoS is adopted. The dashed line indicates the one without magnetic fields.

Downloaded from https://academic.oup.com/ptep/article-abstract/2019/8/083E01/5546028 by CERN - European Organization for Nuclear Research user on 07 September 2019

Table 4. Basic nuclear properties for each EoS. Data are taken from Refs. [9,48].

	GM1	TM1-a	TM1-b	TM2$\omega\rho$-a	TM2$\omega\rho$-b
B/A (MeV)	−16.3	−16.3	−16.3	−16.4	−16.4
ρ_0 (fm^3)	0.153	0.146	0.146	0.146	0.146
K (MeV)	300	281.2	281.2	281.7	281.7
$K_{\rm sym}$ (MeV)	18.1	33.8	33.8	−70.5	−70.5
J (MeV)	32.5	36.9	36.9	32.1	32.1
L (MeV)	94.4	111.2	111.2	54.8	54.8

symmetry energy L has a significant correlation with the radius of a neutron star. Namely, TM2$\omega\rho$ gives the smallest radius for the smallest L and TM1 gives the largest radius for the largest L among the present models. This is in accordance with the results in Refs. [46,47].

5. Summary

In this paper we solved the Einstein equation in axially symmetric space due to the strong poloidal magnetic field in a perturbative approach, which was first introduced by J. B. Hartle. In this work, we used EoSs given in various relativistic mean field theories in the presence of strong magnetic fields. The introduction of Pauli paramagnetism and Landau diamagnetism makes the EoSs considerably stiffer. The mass–radius (MR) relation of neutron stars was calculated by solving the TOV equations with isotropic EoSs (SSMP), or the Hartle equations in the deformed case (PMF). In the PMF case the amount of incremental mass due to the magnetic pressure is suppressed compared with the mass in the SSMP case.

It was previously reported in the calculations of the SSMP case that neutron stars could achieve twice the solar mass for sufficiently strong magnetic fields of the order of 10^{18} G. In the PMF prescription the maximum mass increment is largely suppressed. Therefore twice the solar mass is not achieved even in such strong magnetic fields. Only in the case of TM2$\omega\rho$-b does the mass become $1.99 M_\odot$. The PMF treatment imposes a strong constraint on the EoSs and a restriction on the strength of the magnetic field.

In this work we treated magnetized neutron stars in a perturbative treatment. N. Yasutake et al. [49] discussed rotating neutron stars in the full treatment in an unperturbed method. In future work, this kind of unperturbed method should be tested to investigate the MR relations of neutron stars in the presence of strong magnetic fields.

Acknowledgements

This work was supported by a Grant-in-Aid for Scientific Research (C) (Nos. 16K05341 and 17K05445) from the Japan Society for the Promotion of Science (JSPS).

Appendix A. Energy spectra in strong magnetic fields

Energy spectra for charged baryons, neutral baryons, and leptons with σ, ω, and ρ mesons are derived from the Dirac equation and given by

$$E^b_{\nu,s} = \sqrt{\left(k^b_z\right)^2 + \left(\overline{m}^c_b\right)^2} + g_{\omega b}\omega^0 + \tau_{3b} g_{\rho b}\rho^{03}, \tag{A.1}$$

Downloaded from https://academic.oup.com/ptep/article-abstract/2019/8/083E01/5546028 by CERN - European Organization for Nuclear Research user on 07 September 2019

$$E_s^b = \sqrt{\left(k_z^b\right)^2 + (\overline{m}_b)^2} + g_{\omega b}\omega^0 + \tau_{3b} g_{\rho b}\rho^{03}, \tag{A.2}$$

$$E_\nu^l = \sqrt{\left(k_z^l\right)^2 + (\overline{m}_l)^2}, \tag{A.3}$$

respectively. Here, the effective masses are defined as

$$\overline{m}_b^c = \sqrt{m_b^{*2} + 2\nu|q_b|B} - s\mu_N\kappa_b B, \tag{A.4}$$

$$\overline{m}_b = m_b^* - s\mu_N\kappa_b B, \tag{A.5}$$

$$\overline{m}_l = \sqrt{m_l^2 + 2\nu|q_l|B}, \tag{A.6}$$

for charged baryons, neutral baryons, and leptons, respectively, where

$$m_b^* = m_b - g_{\sigma b}\sigma. \tag{A.7}$$

ν represents the Landau levels

$$\nu = n + \frac{1}{2} - \mathrm{sgn}(q_b)\frac{s}{2} = 0, 1, 2, \ldots, \nu_{\max}, \tag{A.8}$$

where n implies any integer greater than or equal to zero, and $s = +1$ for spin-up and $s = -1$ for spin-down, respectively. Namely, we should vary the lowest values of ν, which takes 0 or 1, depending on the signs of charges and the spin third components. The maximum values of the Landau levels are given by

$$\nu_{\max} = \frac{(E_{\mathrm{F}}^b + s\mu_N\kappa_b B)^2 - m_b^{*2}}{2|q_b|B}, \tag{A.9}$$

$$\nu_{\max} = \frac{(E_{\mathrm{F}}^l)^2 - m_l^2}{2|q_l|B}. \tag{A.10}$$

The Fermi wave numbers $k_{\mathrm{F},\nu,s}^b$, $k_{\mathrm{F},s}^b$, and $k_{\mathrm{F},\nu}^l$ are given by the usual relations

$$(E_{\mathrm{F}}^b)^2 = \begin{cases} (k_{\mathrm{F},\nu,s}^b)^2 + \left(\overline{m}_b^c\right)^2 \\ \\ (k_{\mathrm{F},s}^b)^2 + (\overline{m}_b)^2 \end{cases} \tag{A.11}$$

for baryons and

$$(E_{\mathrm{F}}^l)^2 = (k_{\mathrm{F},\nu}^l)^2 + \overline{m}_l^2 \tag{A.12}$$

for leptons. We then obtain the scalar density and the vector density

$$\rho_b^s = \frac{|q_b|Bm_b^*}{2\pi^2}\sum_s\sum_\nu^{\nu_{\max}} \frac{\overline{m}_b^c}{\sqrt{m_b^{*2} + 2\nu|q_b|B}} \ln\left|\frac{k_{\mathrm{F},\nu,s}^b + E_{\mathrm{F}}^b}{\overline{m}_b^c}\right|, \tag{A.13}$$

$$\rho_b^\nu = \frac{|q_b|B}{2\pi^2}\sum_s\sum_\nu^{\nu_{\max}} k_{\mathrm{F},\nu,s}^b \tag{A.14}$$

for charged baryons,

$$\rho_b^s = \frac{m_b^*}{4\pi^2}\sum_s\left[E_{\mathrm{F}}^b k_{\mathrm{F},s}^b - \overline{m}_b^2 \ln\left|\frac{k_{\mathrm{F},s}^b + E_{\mathrm{F}}^b}{\overline{m}_b}\right|\right], \tag{A.15}$$

Downloaded from https://academic.oup.com/ptep/article-abstract/2019/8/083E01/5546028 by CERN - European Organization for Nuclear Research user on 07 September 2019

$$\rho_b^v = \frac{1}{2\pi^2}\sum_s \left[\frac{1}{3}\left(k_{\mathrm{F},s}^b\right)^3 - \frac{1}{2}s\mu_N\kappa_b B\left\{\overline{m}_b k_{\mathrm{F},s}^b + \left(E_{\mathrm{F}}^b\right)^2\left(\arcsin\left(\frac{\overline{m}_b}{E_{\mathrm{F}}^b}\right) - \frac{\pi}{2}\right)\right\}\right] \tag{A.16}$$

for neutral baryons, and

$$\rho_l^v = \frac{|q_l|B}{2\pi^2}\sum_s \sum_{\nu}^{\nu_{\max}} k_{\mathrm{F},\nu}^l \tag{A.17}$$

for leptons, respectively.

References

[1] P. B. Demorest, T. Pennucci, S. M. Ransom, M. S. E. Roberts, and J. W. T. Hessels, Nature **467**, 1081 (2010).
[2] J. Antoniadis et al., Science **340**, 1233232 (2013).
[3] D. T. Loan, N. H. Tan, D. T. Khoa, and J. Margueron, Phys. Rev. C **83**, 065809 (2011).
[4] D. Logoteta, I. Vidaña, I. Bombaci, and A. Kievsky, Phys. Rev. C **91**, 064001 (2015).
[5] N. K. Glendenning, Nucl. Phys. A **493**, 521 (1989).
[6] N. K. Glendenning and S. A. Moszkowski, Phys. Rev. Lett. **67**, 2414 (1991).
[7] Y. Sugahara and H. Toki, Nucl. Phys. A **579**, 557 (1994).
[8] K. Tsubakihara and A. Ohnishi, Nucl. Phys. A **914**, 438 (2013).
[9] M. Fortin, S. S. Avancini, C. Providência, and I. Vidaña, Phys. Rev. C **95**, 065803 (2017).
[10] K. Hebeler, J. M. Lattimer, C. J. Pethick, and A. Schwenk, Phys. Rev. Lett. **105**, 161102 (2010).
[11] I. Tews, T. Krüger, K. Hebeler, and A. Schwenk, Phys. Rev. Lett. **110**, 032504 (2013).
[12] T. Krüger, I. Tews, K. Hebeler, and A. Schwenk, Phys. Rev. C **88**, 025802 (2013).
[13] S. Gandolfi, A. Yu. Illarionov, S. Fantoni, J. C. Miller, F. Pederiva, and K. E Schmidt, Mon. Not. R. Astron. Soc. **404**, L35 (2010).
[14] S. Gandolfi, J. Carlson, and S. Reddy, Phys. Rev. C **85**, 032801(R) (2012).
[15] A. W. Steiner and S. Gandolfi, Phys. Rev. Lett. **108**, 081102 (2012).
[16] S. A. Olausen and V. M. Kaspi, Astrophys. J. Suppl. **212**, 6 (2014).
[17] A. Broderick, M. Prakash, and J. M. Lattimer, Astrophys. J. **537**, 351 (2000).
[18] G.-J. Mao, A. Iwamoto, and Z.-X. Li, Chin. J. Astron. Astrophys. **3**, 359 (2003).
[19] J. Dong, W. Zuo, and J. Gu, Phys. Rev. D **87**, 103010 (2013).
[20] A. Rabhi, M. A. Pérez-García, C. Providência, and I. Vidaña, Phys. Rev. C **91**, 045803 (2015).
[21] D. P. Menezes, M. Benghi Pinto, S. S. Avancini, A. Pérez Martínez, and C. Providência, Phys. Rev. C **79**, 035807 (2009).
[22] D. P. Menezes, M. Benghi Pinto, S. S. Avancini, and C. Providência, Phys. Rev. C **80**, 065805 (2009).
[23] V. Dexheimer, R. Negreiros, and S. Schramm, Eur. Phys. J. A **48**, 189 (2012).
[24] R. H. Casali, L. B. Castro, and D. P. Menezes, Phys. Rev. C **89**, 015805 (2014).
[25] P. Markey and R. J. Tayler, Mon. Not. R. Astron. Soc. **163**, 77 (1973).
[26] P. Markey and R. J. Tayler, Mon. Not. R. Astron. Soc. **168**, 505 (1974).
[27] J. Braithwaite, Astron. Astrophys. **469**, 275 (2007).
[28] J. Braithwaite, Mon. Not. R. Astron. Soc. **397**, 763 (2009).
[29] M. Bocquet, S. Bonazzola, E. Gourgoulhon, and J. Novak, Astron. Astrophys. **301**, 757 (1995).
[30] C. Y. Cardall, M. Prakash, and J. M. Lattimer, Astrophys. J. **554**, 322 (2001).
[31] J. B. Hartle, Astrophys. J. **150**, 1005 (1967).
[32] J. B. Hartle and D. H Sharp, Astrophys. J. **147**, 317 (1967).
[33] J. B. Hartle and K. S. Thorne, Astrophys. J. **153**, 807 (1968).
[34] S. Chandrasekhar and J. C. Miller, Mon. Not. R. Astron. Soc. **167**, 63 (1974).
[35] R. Mallick and S. Schramm, Phys. Rev. C **89**, 045805 (2014).
[36] N. K. Glendenning, *Compact Stars: Nuclear Physics, Particle Physics and General Relativity* (Springer, Berlin, 2012).
[37] A. F. Fantina, N. Chamel, Y. D. Mutafchieva, Zh. K. Stoyanov, L. M. Mihailov, and R. L. Pavlov, Phys. Rev. C **93**, 015801 (2016).
[38] G. Baym, C. Pethick, and P. Sutherland, Astrophys. J. **170**, 299 (1971).

Downloaded from https://academic.oup.com/ptep/article-abstract/2019/8/083E01/5546028 by CERN - European Organization for Nuclear Research user on 07 September 2019

[39] G. Audi, M. Wang, A. H. Wapstra, F. G. Kondev, M. MacCormick, X. Xu, and B. Pfeiffer, Chin. Phys. C **36**, 1287 (2012).
[40] M. Wang, G. Audi, A. H. Wapstra, F. G. Kondev, M. MacCormick, X. Xu, and B. Pfeiffer, Chin. Phys. C **36**, 1603 (2012).
[41] S. Goriely, N. Chamel, and J. M. Pearson, Phys. Rev. C **88**, 024308 (2013).
[42] D. Bandyopadhyay, S. Chakrabarty, and S. Pal, Phys. Rev. Lett. **79**, 2176 (1997).
[43] C. Patrignani et al. [Particle Data Group], Chin. Phys. C **40**, 100001 (2016).
[44] L. Lopes and D. Menezes, J. Cosmol. Astropart. Phys. **1508**, 002 (2015).
[45] D. P. Menezes and L. L. Lopes, Eur. Phys. J. A **52**, 17 (2016).
[46] S. S. Bao, J. N. Hu, Z. W. Zhang, and H. Shen, Phys. Rev. C **90**, 045802 (2014).
[47] X. Wu, A. Ohnishi, and H. Shen, Phys. Rev. C **98**, 065801 (2018).
[48] M. Fortin, C. Providência, Ad. R. Raduta, F. Gulminelli, J. L. Zdunik, P. Haensel, and M. Bejger, Phys. Rev. C **94**, 035804 (2016).
[49] N. Yasutake, K. Fujisawa, and S. Yamada, Mon. Not. R. Astron. Soc. **463**, 3705 (2016).

Downloaded from https://academic.oup.com/ptep/article-abstract/2019/8/083E01/5546028 by CERN - European Organization for Nuclear Research user on 07 September 2019